Communication

1064/1319 nm Dual-Wavelength Alternating Electro-Optic Q-Switched Laser Based on the Common Q-Switching Bias Voltage

Jingdong Sun, Chunhe Yu, Yuan Dong *, Chunting Wu and Guangyong Jin

Jilin Key Laboratory of Solid-State Laser Technology and Application, School of Physics, Changchun University of Science and Technology, Changchun 130022, China; 2019200002@mails.cust.edu.cn (J.S.); yuchunhe@mails.cust.edu.cn (C.Y.); bigsnow@cust.edu.cn (C.W.); jgyciom@cust.edu.cn (G.J.)
* Correspondence: dongyuan@cust.edu.cn

Abstract: A dual-wavelength alternating electro-optic (EO) Q-switched laser operating at 1064 and 1319 nm is designed, which takes the structure of double the gain crystals and a single EO modulator with the common Q-switching bias voltage (CQBV). The output characteristics of alternating dual-wavelength pulse lasers are studied via simulations and experiments. The results show that the energy ratio of the two lasing wavelengths can be controlled by changing the CQBV. This is because the CQBV affects the loss of two resonators, 1064 and 1319 nm, at the same time. The gain–loss relationship in the dual-wavelength laser resonators can be controlled by changing the CQBV in a certain range.

Keywords: dual-wavelength laser; EO Q-switched; gain–loss relationship; energy ratio

1. Introduction

Compared with the dual-wavelength pulse laser achieved by acoustic-optic or passive Q-switched technology, the dual-wavelength pulse laser obtained by EO Q-switched technology has the virtues of high peak power, high stability and a narrower pulse width. Based on this, EO Q-switched dual-wavelength lasers have wide applications in non-linear frequency conversion, laser drilling, laser spectroscopy, laser ranging and other fields [1–5]. However, at present, the dual-wavelength pulse lasers obtained by EO Q-switched technology are output at the same time, which greatly limits its applications [6–8]. For example, dual-wavelength pulse lasers with a time delay are required to act on metal samples one after another in laser-induced breakdown spectroscopy (LIBS). Since LIBS using a dual-wavelength laser emitted at the same time cannot separate the two processes of laser stripping and plasma induction, the sensitivity of sample analysis is low. Once a certain element has a relatively low content in the sample to be tested, it cannot be detected. However, for the dual-wavelength alternating pulse lasers, the first pulse is used to peel off the sample, and the high-temperature plasma is excited. When the plasma plume begins to cool down, the second pulse is used as the excitation light source of the sample. At the same time, the plasma generated by the first pulse is also re-excited. The dual-wavelength pulse lasers are separated in the time domain. As a result, the two processes of laser stripping and the subsequent excitation of the sample are separated in time [9–11]. The atomic emission spectrum is enhanced. The sensitivity of spectral analysis is improved [12,13]. That is to say, compared with LIBS using a dual-wavelength laser emitted at the same time, LIBS using a dual-wavelength laser with a time delay has a lower detection limit for elements. As a result, elements with a relatively low content in the sample are also reported [14,15]. However, to improve the spatial resolution and sensitivity of sample detection, it is essential to control the energy ratio of the alternating dual-wavelength pulse lasers [16].

There are several ways to control the output energy ratio of two pulse lasers, such as controlling the energy ratio by setting the transmittance of the two lasing wavelengths

at the output mirror. The disadvantage of this method is that it is difficult to get the best coating results because of the influence of the coating accuracy at home and abroad. In addition, due to the long coating period, it is difficult to change once the coating parameters are determined, which is not conducive to the rapid adjustment of laser experiments. Then, the energy ratio can also be controlled by changing the resonator length of the two lasing wavelengths. However, it is hard to reach the accuracy of the theoretical calculation by manually adjusting the length of the resonator. Alternatively, the energy ratio can also be controlled by changing the voltage of EO modulator.

In 2015, Men S. et al. achieved 1047 nm and 1053 nm dual-wavelength pulse lasers output using double Nd:YLF crystals pumped by a xenon lamp and a single EO modulator. While the λ/4 high voltage was loaded on the EO crystal, the maximum energies of 1047 nm and 1053 nm are 66.2 mJ and 83.9 mJ. The two laser pulse widths were both 18 ns [17]. In 2021, Wang C. et al. obtained 1064 and 1342 nm dual-wavelength lasers output by utilizing the structure of a single laser crystal combined with a double RbTiOPO$_4$(RTP) EO modulator. The dual-wavelength pulse lasers output with a power ratio of 1:1 was realized by adjusting the voltages of two Q-switched crystals. When the voltage was 2000 V for 1064 nm and 1920 V for 1342 nm, respectively, the dual-wavelength pulse lasers with 1.6 W output power were obtained at 10 kHz repetition and 30 W injection power. The pulse widths of 1064 and 1342 nm were 42 and 81 ns, respectively [18]. It can be concluded that the output energy ratio can be controlled by changing the voltage loaded on the shared EO modulator for the dual-wavelength lasers with a small wavelength difference. Since the wavelength difference is small, there is a similar quarter-wavelength Q-switching voltage for the dual-wavelength lasers. The energy ratio can be adjusted between the two optimal crystal voltages. However, there is a great distinction between the quarter-wavelength Q-switching voltage and the stimulated-emission cross-section for the two wavelengths with a large wavelength difference. It is very difficult to choose a common voltage that can not only Q-switch the dual-wavelength lasers at the same time but also adjust the output energy ratio of the two wavelength components. Therefore, only two EO modulators can be selected to correspondingly Q-switch the dual-wavelength lasers. The energy ratio is controlled by adjusting the two Q-switching voltages on the double Q-switched crystals. In addition, if the dual-wavelength lasers use double Q-switches for Q-switching, a single laser crystal is generally used to emit the dual-wavelength lasers. At this time, there is a serious gain competition between the two wavelengths.

In this study, a dual-wavelength alternating EO Q-switched laser is established. The structure of a single Q-switcher with the CQBV shared by two laser gain mediums is used. The dual-wavelength lasers are emitted by two gain mediums. In addition, there is no gain line competition between them. Adjusting the CQBV in a certain range can not only control the energy ratio of the alternating dual-wavelength pulses but also alternately Q-switch the two wavelength components. In addition, the alternating dual-wavelength pulses have a time delay in the time domain. The time interval is adjustable. The results can provide a reliable illumination source for the field of LIBS.

2. Theoretical Simulation and Analysis

To understand the alternate emission process of 1064 and 1319 nm lasers, a model of a dual-wavelength alternating EO Q-switched laser based on the CQBV is established as follows [19]:

$$\frac{dn_i}{dt_i} = R_{pi} - n_i\sigma_i\varnothing_i c\gamma - \frac{n_i}{\tau_f} \tag{1}$$

$$\frac{d\varnothing_i}{dt_i} = \varnothing_i\left(n_i\sigma_i c - \frac{1}{\tau_{ci}}\right) i = 1,2 \tag{2}$$

$$t_1 = \Delta t + (n-1)T\left(\Delta t + (n-1)T \le t_1 \le \Delta t + \Delta\tau_1 + (n-1)T\right) \tag{3}$$

$$t_2 = t_1 + \Delta t \; (2\Delta t + (n-1)\mathrm{T} \le t_2 \le 2\Delta t + \Delta\tau_2 + (n-1)\mathrm{T}) \tag{4}$$

where n_1 and n_2 are the inverse populations in the upper level of the 1319 and 1064 nm lasers. $\varnothing_1$ and $\varnothing_2$ are the laser photon density of the 1319 nm and 1064 nm lasers, respectively. R_{p1} and R_{p2} are the pumping rates for 1319 nm and 1064 nm, respectively. c is the speed of light. σ_1 and σ_2 are the stimulated-emission cross-sections for the 1319 and 1064 nm lasers, respectively. γ is the inversion factor. Δt represents the time delay between the two alternating components. $\Delta\tau_1$ and $\Delta\tau_2$ represent the pulse widths for 1319 nm and 1064 nm, respectively. T represents the EO Q-switched period. τ_f is the lifetime of the upper level of Nd:YAG. In the 1319 and 1064 nm laser cavities, the photon decay time τ_{ci} is shown as

$$\tau_{ci} = \frac{2l_{ci}}{c\delta_i} \; i = 1,2 \tag{5}$$

$$\delta_i = T_0 - \ln(R_i) + L_{Qi}(t) \tag{6}$$

$$L_{Q1}(t) = -ln\left[sin^2(\frac{\pi V_{(t)}}{2V_{1319/4}}) \right] \tag{7}$$

$$L_{Q2}(t) = -ln\left[cos^2(\frac{\pi V_{(t)}}{2V_{1064/4}}) \right] \tag{8}$$

$$V_{(t)} = \begin{cases} 0 & (t < \Delta t + (n-1)T) \\ V_1 & (\Delta t + (n-1)T \le t \le 2\Delta t + (n-1)T) \\ 0 & (t > 2\Delta t + (n-1)T) \end{cases} \tag{9}$$

where l_{c1} and l_{c2} are the lengths of the 1319 and 1064 nm laser cavities, respectively. δ_1 and δ_2 are the total losses of the 1319 and 1064 nm lasers, respectively. T_0 is the dissipative loss. R_1 and R_2 are the reflectivities of the 1319 and 1064 nm lasers, respectively, at the output coupler. $-\ln(R_1)$ and $-\ln(R_2)$ are the coupling losses of the 1319 and 1064 nm lasers, respectively. $L_{Q1}(t)$ and $L_{Q2}(t)$ represent the Q-switched losses for the 1319 and 1064 nm laser cavities, respectively. $V_{1319/4}$ and $V_{1064/4}$ are the $\lambda/4$ voltages for 1319 and 1064 nm, with values of 1500 V and 1200 V, respectively. $V_{(t)}$ is the CQBV applied on or removed from the shared Q-switcher, which changes with time.

Whether the CQBV can alternately Q-switch for two wavelengths depends on the relationship between the total loss and gain in the 1319 and 1064 nm laser resonators. Then, the gain of the two laser resonators can be calculated according to Equation (10) [20].

$$G_i = \varepsilon_i R_{1i} R_i \exp(2\sigma_i n_{0i} l) \; (i = 1,2) \tag{10}$$

$$n_{0i} = R_{pi}\tau_f \left[1 - \exp(-t_0/\tau_f) \right] \tag{11}$$

where G_1 and G_2 are the gain of the 1319 and 1064 nm lasers, respectively. ε_1 and ε_2 are the loss terms of the 1319 and 1064 nm lasers, respectively. R_{11} and R_{12} are the reflectivities of the 1319 and 1064 nm lasers at the total reflector mirror, respectively. n_{01} and n_{02} are the initial inverse populations, which can be calculated according to Equation (11). t_0 is the Q-switched time. l is the length of the Nd:YAG rod.

For the dual-wavelength alternating EO Q-switched laser, two laser gain mediums are used to emit dual-wavelength lasers. In addition, the 1064 and 1319 nm lasers share the single EO modulator with the CQBV. The CQBV is used to alternately Q-switch the dual-wavelength lasers. The 1319 nm laser adopts a voltage-increased EO Q-switch by using the rising edge of the CQBV, while the 1064 nm laser adopts a voltage-decreased EO Q-switch by using the falling edge of the CQBV. Therefore, the temporal interval between the two wavelength components is 200 us, corresponding to the duration of the Q-switching

bias voltage. If the CQBV can completely and alternately Q-switch the two lasers, it should ensure two points. On the one hand, when the CQBV is applied, a 1319 nm pulse laser is obtained. However, the high voltage lasts 200 μs. In addition, the pumping source of 1064 nm is also working in the 200 μs maintained by the high voltage. Therefore, not only does the gain of the 1319 nm resonator need to be greater than the total loss, but the gain of the 1064 nm resonator also needs to be less than the total loss when the CQBV is applied. In this way, only the 1319 nm pulse laser is output when the common Q-switching voltage is applied. That is to say, the shared EO modulator should turn on 1319 nm and turn off 1064 nm at the same time. On the other hand, when the CQBV is removed (the CQBV is equal to 0), the 1064 nm pulse laser is obtained. However, within the time when the CQBV is 0, the pumping source of the 1319 nm laser is also working at the same time. Therefore, not only does the gain of the 1064 nm resonator need to be greater than the total loss but also the gain of the 1319 nm resonator needs to be less than the total loss when the CQBV is removed. In this way, only the 1064 nm pulse laser is output when the common Q-switching voltage is removed. That is to say, the shared EO modulator should turn on 1064 nm and turn off 1319 nm at this time. Based on these two aspects, Figure 1 shows the numerical simulation of the relationship between the CQBV and the gain/loss in the two resonators. The parameters used in the theoretical calculation are given in Table 1 [21–23].

When the CQBV is applied, the shared EO modulator turns on the 1319 nm laser when the CQBV is in the range of 819–2181 V. When the CQBV is in the range of 877–1524 V, the shared EO modulator turns the 1064 nm laser off. In addition, it can be seen from Figure 1 that when the CQBV is removed (meaning the CQBV is equal to 0), the 1319 nm laser gain is less than the total loss. In addition, the 1064 nm total loss is less than the gain. Therefore, the CQBV that can alternately Q-switch dual-wavelength lasers ranges from 877 V to 1524 V. Then, the rate equation of the dual-wavelength alternating EO Q-switched laser is numerically solved by making use of the fourth-order Runge–Kutta method, with the CQBV shared by the dual-wavelength laser as the boundary condition. The photon number density versus time when the CQBV is at 899 V, 1200 V, 1453 V and 1500 V is shown in Figure 2.
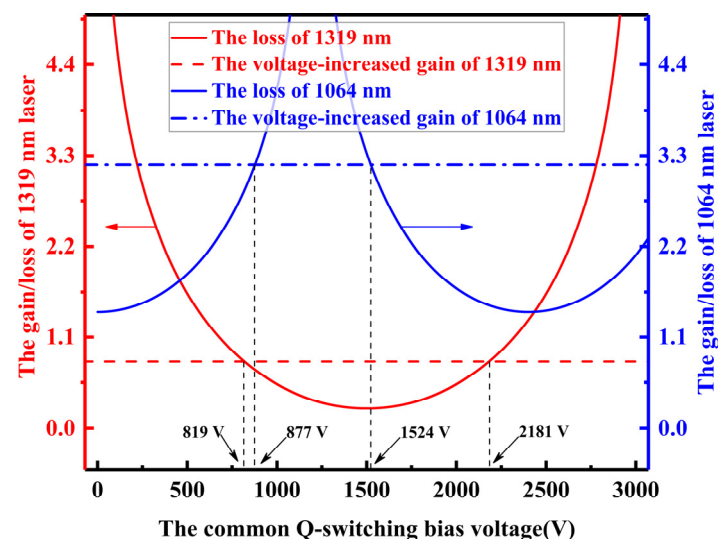

Figure 1. The relationship between gain/loss and the CQBV in 1064 and 1319 nm laser resonators.

As shown in Figure 2, the peak photon number density of the 1319 nm laser is positively correlated with the CQBV. The peak photon number density of the 1064 nm laser increases at first and then decreases with the increase in the CQBV. When the CQBV is 1200 V, the peak photon number density of the 1064 nm laser reaches the maximum. In addition, when the CQBV is less than 1453 V, the peak photon density ratio of the 1319/1064 nm laser is less than 1. When the CQBV is 1500 V, the peak photon density

ratio of the 1319/1064 nm laser is greater than 1. The simulation result shows that the photon number density ratio of the two wavelengths of the 1319/1064 nm laser reaches 1:1 when the CQBV ranges from 1453 V to 1500 V. This provides an effective way to realize the 1:1 output energy ratio of the dual-wavelength alternating Q-switched laser based on the CQBV.

Table 1. The parameters of the numerical simulation.

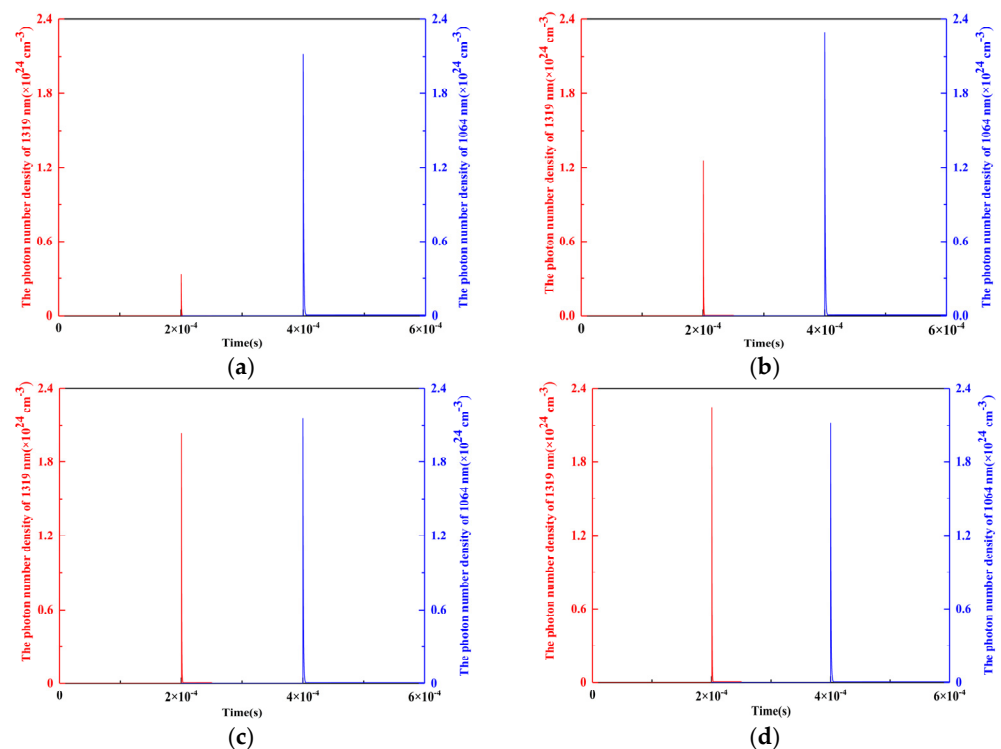| Definition (Unit), Parameters	Value	Definition (Unit), Parameters	Value
Dissipative loss, T_0	0.02	Stimulated-emission cross-section of 1319 nm ($\times 10^{-19}$ cm^2), σ_1	0.56
Output mirror reflectivity of 1319 nm, R_1	0.8	Stimulated-emission cross-section of 1064 nm ($\times 10^{-19}$ cm^2), σ_2	2.8
Output mirror reflectivity of 1064 nm, R_2	0.25	Inversion factor, γ	1
Pumping rate of 1319 nm ($\times 10^{27}$ m^{-3}/s), R_{p1}	2.42	The velocity of light ($\times 10^8$ m/s), c	3
Pumping rate of 1064 nm ($\times 10^{26}$ m^{-3}/s), R_{p2}	9.46	Q-switched time (μs), t_0	200
Quarter wavelength voltage of 1319 nm (V), $V_{1319/4}$	1500	Spontaneous lifetime (μs), τ_f	230
Quarter wavelength voltage of 1064 nm (V), $V_{1064/4}$	1200	The length of Nd:YAG (mm), *l*	80

Figure 2. The photon number density versus time when the CQBV is at (taking the first pulse of the dual−wavelength laser as a reference) (**a**) 899 V; (**b**) 1200 V; (**c**) 1453 V; (**d**) 1500 V.

3. Experimental Setup

The experimental setup of the 1064 and 1319 nm dual-wavelength alternating EO Q-switched lasers based on the CQBV is shown in Figure 3. An alternating output for the 1064 and 1319 nm dual-wavelength pulse lasers is achieved by making use of the double-cavity structure of, the double laser crystals and a single EO Q-switcher. The linear resonator provides the optical feedback and laser output for 1319 nm, whereas the folded cavity

provides the optical feedback and laser output for 1064 nm. A single EO modulator with the CQBV and an output mirror are shared by two resonators for both components. The linear resonator, with a length of 26.9 cm, is made up of M1, an Nd : YAG (for 1319 nm) rod, P1, C1, a Q-switcher and M5. The folded cavity, with a length of 30 cm, is made up of M3, an Nd : YAG (for 1064 nm) rod, P2, M4, M2, a Q-switcher and M5. M1 is the plano-concave total reflective mirror with the coated parameters of high reflectivity (HR)@1319 nm (R > 99%) and high transmission (HT)@1064 nm (T > 99%) on the concave side. M3 is the plano-concave total reflective mirror with the coated parameter of HR@1064 nm on the concave side (R > 99%). The doping concentration and the size are the same for Nd : YAG (for 1064 nm) and Nd : YAG (for 1319 nm). The concentration of Nd^{3+} in Nd:YAG is 0.6 at.%. The crystal size is $\phi 4 \times 80$ mm. The HT coatings for 1064 and 1319 nm are plated on the ends (R < 0.5%). Two Nd:YAG rods are unilateral-side-pumped by two 808 nm laser diode (LD) stacked arrays. The pumping light passes through a U-shaped condenser cavity into an Nd:YAG crystal. The LD stacked array contains four stacked blocks. In addition, each stacked block is composed of 10 single bars. The stacked array pumping power is 3600 W. The TEC temperature controller is used to keep two LD stacked arrays at a constant temperature of 323 K. The two LD stacked arrays are powered by two laser power supplies. P1 and P2 are polarizers. C1 is a quarter-wave plate. The coated parameters of 45° mirror M2 are that the left surface S1 is plated with HT@1319 nm and the right surface S2 is plated with HT@1319 nm and HR@1064 nm. Moreover, M4 is a 45° mirror with the coated parameter of HR@1064 nm (R > 99%). M5 is the output mirror with a double-sided coated. The parameter of the left surface S1 is anti-refletance@1064 + 1319 nm (T > 99%), and the right surface S2 is coated with dichroic film with transmittance of 75% for 1064 nm and transmittance of 20% for 1319 nm. In order to compensate for the natural birefringence effect of the RTP crystal caused by temperature, two identical orthogonal RTP crystals are employed as the shared EO modulator [24,25]. The dimensions of the two x-cut RTP crystals are $6 \times 6 \times 10$ mm^3. The films of HT@(1064 + 1319)nm are coated on both end faces of the RTP crystals. The two RTP crystals are parallel to each other along the z-axis (the direction of light passing). Furthermore, the x-axis of one of the two RTP crystals is parallel to the y-axis of the other. That is, the two RTP crystals rotate 90° relative to each other. The two x–z faces perpendicular to the y-axis of each RTP modulator are the electrodes of the common EO modulator. The three-dimensional diagram of the shared EO modulator is shown in Figure 4.
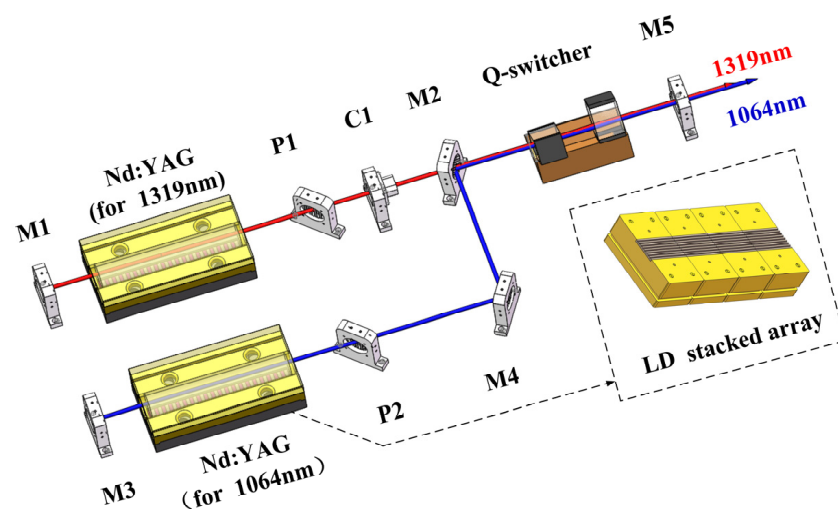

Figure 3. Experimental setup of 1064 and 1319 nm dual-wavelength alternating EO Q-switched lasers.
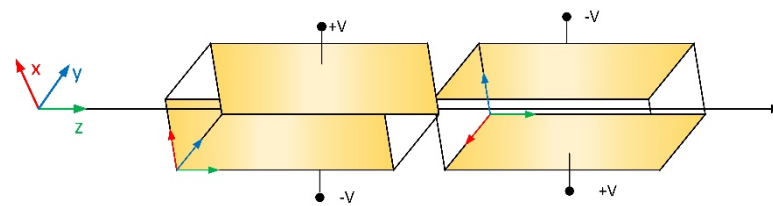
Figure 4. The three−dimensional diagram of the shared EO modulator.

Moreover, the alternating output of the 1064 and 1319 nm pulses depends not only on the structure design, as shown in Figure 3, but also on the timing relationship of the driving signals among the RTP crystals, the pumping source for 1064 nm and the pumping source for 1319 nm. The timing control relationship of the three driving signals is shown in Figure 5.
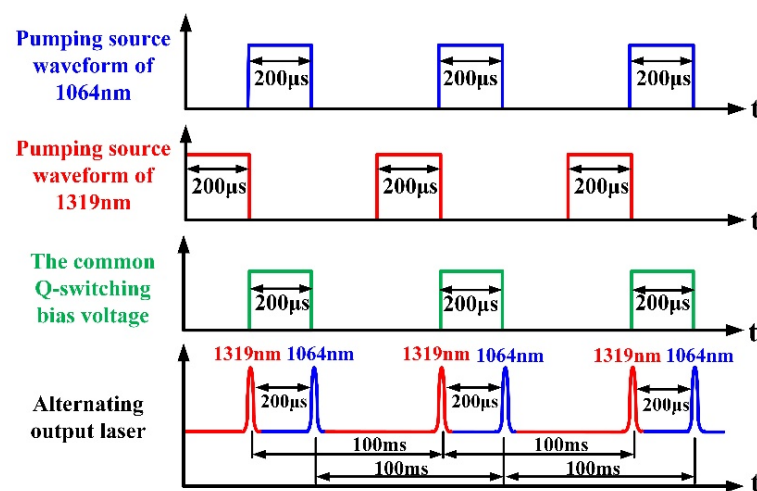

Figure 5. The temporal relation of driving signals among RTP modulator and pumping sources for 1064 and 1319 nm.

The two Nd:YAG rods are alternately pumped by two LD stacked arrays on the unilateral side. Every gain media is pumped by the pumping source with a 100 ms interval and a 200 μs pumping duration. The pumping source of the 1319 nm laser starts pumping at first. From the structure shown in Figure 3, it can be seen that the voltage-increased EO Q-switched technology is adopted by 1319 nm and the voltage-decreased EO Q-switched technology is utilized by 1064 nm. Therefore, the 1319 nm resonator is under high loss when the shared Q-switcher is not loaded with the CQBV in 0–200 μs. Then, the 1319 nm pulse is obtained by loading the CQBV at 200 μs. The gain medium of 1064 nm is under population inversion when the shared EO modulator is loaded with the CQBV in 200–400 μs. When the CQBV is removed from the shared EO modulator at 400 μs, the 1064 nm pulse laser lagged behind the 1319 nm pulse laser at 200 μs in the time domain that is achieved. In addition, the dual-wavelength alternating EO Q-switched laser is equipped with tuning software. It is mainly used to control the timing sequence relationship among the driving signals of the 1064 and 1319 nm laser power supplies and the EO crystal driver module. By adjusting the trigger time, relative delay time and duration of the three signals, the temporal interval between the two wavelength components can be tuned.

During the experiment, the CQBV applied to the shared Q-switcher can be adjusted by the EO crystal driver module to gain the alternating output of the 1064 and 1319 nm dual-wavelength pulse lasers.

4. Experimental Results and Discussion

After collimating the optical path, the working frequency of the laser is set to 10 Hz. According to the numerical simulation result, the alternate Q-switching range of the CQBV

is from 877 V to 1524 V. Therefore, the CQBV applied to the shared EO modulator is selected to be 1100 V. First, the output spectrum is recorded by using a spectrometer (AvaSpec-2048-USB2, Avantes) under the injection energy of 260 mJ for 1064 nm and the injection energy of 665 mJ for 1319 nm. The wavelengths of the two pulse lasers are 1064 nm and 1319 nm, as illustrated in Figure 6. Then, the two lasing components are separated outside the cavity by using a spectroscope. Under the same repetition frequency, CQBV and injection pumping energy conditions, the sequences of the dual-wavelength lasers are measured by using the method of connecting two photodetectors (DET 10 D/M, DET 10 A/M, Thorlabs) to two channels of the same oscilloscope (DPO7104C, Tektronix). Figure 7a shows that both 1064 and 1319 nm are output at the repetition frequency of 10 Hz. As shown in Figure 7b, the dual-wavelength lasers are separated in the time domain by amplifying any group of dual-wavelength pulsed lasers. The 1064 nm and 1319 nm are alternately output. The 1319 nm pulse takes the lead in output, while the 1064 nm pulse lags behind the 1319 nm pulse at 200 µs.

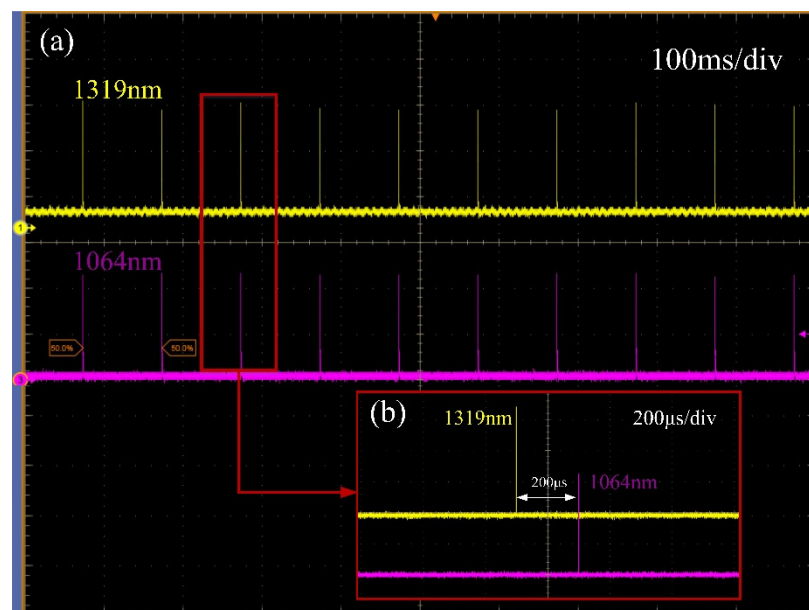**Figure 6.** The spectrogram of the dual-wavelength alternating EO Q-switched laser.

Figure 7. Alternating sequence of 1064 and 1319 nm pulses. (**a**) 1064 and 1319 nm pulse trains; (**b**) 1064 and 1319 nm dual-wavelength lasers alternating output at intervals of 200 µs.

Finally, when the injection energies of the 1064 and 1319 nm lasers are 260 mJ and 665 mJ, respectively, the output characteristics of dual-wavelength alternating EO Q-switched laser are recorded when the CQBV is at different voltages. As shown in Figure 8, the range of the CQBV that can alternately turn off the Q-switch for two lasers is 829 V to 1487 V. Although the Q-switching length is 658 V, the different common Q-switching bias voltages correspond to the different output characteristics of the two pulse lasers. The energy of the 1064 nm pulse increases at first and then decreases with the increase in the CQBV. The energy of the 1064 nm pulse reaches the peak when the CQBV is 1200 V. In addition, the maximum energy is 43 mJ. The energy of the 1319 nm pulse is positively correlated with the CQBV. The energy of the 1319 nm pulse reaches the peak when the CQBV is 1487 V. Moreover, the maximum energy is 40.1 mJ. It can be seen that the energy of the two lasers varies with the CQBV. This is because when the CQBV changes, the Q-switching loss in the two resonators also changes, which affects the dual-wavelength laser output characteristics. The wavelength difference (255 nm) between 1064 nm and 1319 nm is large. The stimulated-emission cross-section (5:1) and the quarter-wavelength voltage (1200 V@1064 nm, 1500 V@1319 nm) are also different. Despite the above differences between the two lasing components, a range of the CQBV can still be found that can alternately Q-switch the dual-wavelength lasers. In addition, the loss in the two resonators can be controlled by optimizing the CQBV to control the output characteristics of the two lasing components. When the CQBV is 1487 V, the output energy of 1064 nm is 40.13 mJ, which is approximate to the output single pulse energy of 40.1 mJ for 1319 nm. In addition, a 1:1 ratio of the output single pulse energy is obtained. When the output energies are 40.13 and 40.1 mJ, the pulse widths of 1064 and 1319 nm are 13.62 and 14.57 ns, respectively, as shown in Figure 9. Figure 10 shows the stability of the energy of the two wavelengths. The energy stabilities of the 1064 and 1319 nm lasers are 0.1% and 0.76%, respectively.
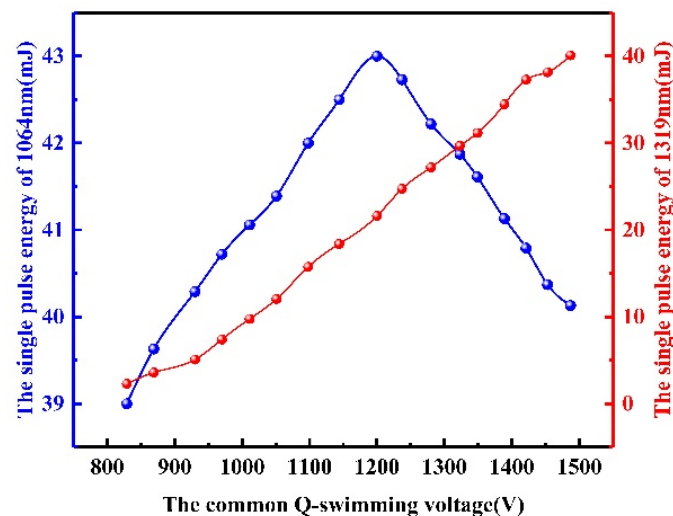

Figure 8. Schematic diagram of 1064 and 1319 nm output energy when the CQBV is adjusted.

The existing dual-wavelength EO Q-switched lasers can only use one of the voltage-increased EO Q-switched technology and the voltage-decreased EO Q-switched technology. The dual-wavelength pulse laser is output at the same time, which cannot be actively regulated. In other words, the time delay between the two signals is zero. Compared with the existing dual wavelength EO Q-switched lasers, the dual wavelength laser with common Q-switching voltage proposed in this paper skillfully combines voltage-increased and voltage-decreased EO Q-switched technologies. The dual wavelength pulse laser is separated in the time domain and is alternately output. Moreover, the time delay between the two signals can be adjusted.
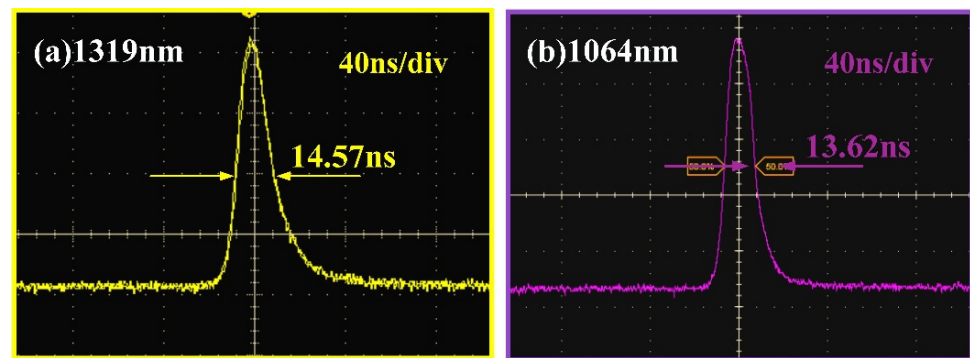
Figure 9. Diagrams of 1064 and 1319 nm dual-wavelength laser pulse widths. (**a**) the pulse width of 1319 nm; (**b**) the pulse width of 1064 nm.
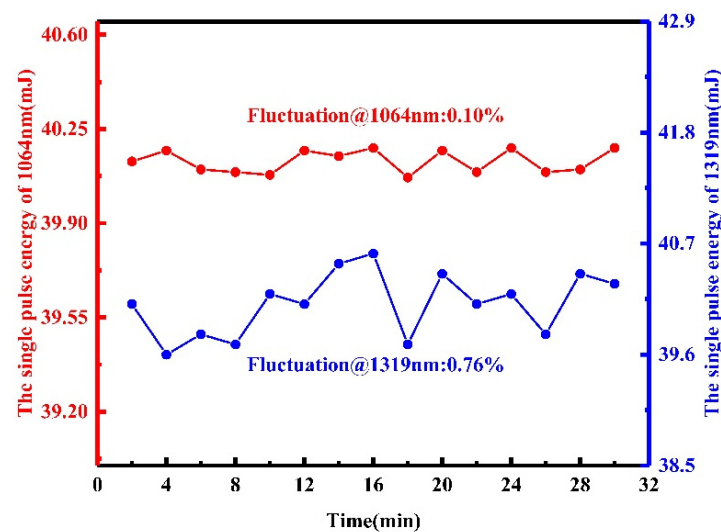

Figure 10. The stability of energy of 1064 and 1319 nm.

5. Conclusions

In summary, an all-solid-state Nd : YAG laser with alternating dual wavelengths of 1064 and 1319 nm is designed. A structure with double the gain crystals and a single common EO modulator with the CQBV is built. A rate equation model of the dual-wavelength alternating EO Q-switched laser based on the CQBV is established. It is theoretically and experimentally proven that the output energy ratio of the dual-wavelength alternating pulse lasers can be controlled by adjusting the CQBV. At a repetition frequency of 10 Hz, the range of the CQBV that can alternately Q-switch for two lasers is 829 V to 1487 V when the injection energy is 260 and 665 mJ for 1064 and 1319 nm, respectively. The output of the alternating dual-wavelength pulse lasers with an energy ratio of 1:1 is obtained when the CQBV is 1487 V. The output energies of 1064 and 1319 nm are 40.13 mJ and 40.1 mJ, respectively. At this time, the pulse widths of 1064 and 1319 nm are 13.62 and 14.57 ns, respectively. The results provide a reliable illumination source for the field of LIBS.

References

1. You, Z.Y.; Zhu, Z.J.; Sun, Y.J.; Huang, Y.S.; Lee, C.K.; Wang, Y.; Li, J.F.; Tu, C.Y.; Lin, Z.B. Simultaneous Q-switched orthogonally polarized dual-wavelength Yb^{3+}:$GdMgB_5O_{10}$ laser. *Opt. Mater. Express* **2017**, *7*, 2760–2766. [CrossRef]
2. Wang, Z.P.; Liu, H.; Wang, J.Y.; Lv, Y.H.; Sang, Y.H.; Lan, R.J.; Yu, H.H.; Xu, X.G.; Shao, Z.S. Passively Q-switched dual-wavelength laser output of LD-end-pumped ceramic Nd:YAG laser. *Opt. Express* **2009**, *17*, 12076–12081. [CrossRef] [PubMed]
3. Song, Q.; Wang, G.J.; Zhang, B.Y.; Wang, W.J.; Wang, M.H.; Zhang, Q.L.; Sun, G.H.; Bo, Y.; Peng, Q.J. Diode-pumped passively dual-wavelength Q-switched Nd:GYSGG laser using graphene oxide as the saturable absorber. *Appl. Opt.* **2015**, *54*, 2688–2692. [CrossRef] [PubMed]
4. Zuo, Z.Y.; Dai, S.B.; Zhu, S.Q.; Yin, H.; Li, Z.; Chen, Z.Q. Power scaling of an actively Q-switched orthogonally polarized dual-wavelength Nd:YLF laser at 1047 and 1053 nm. *Opt. Lett.* **2018**, *43*, 4578–4581. [CrossRef] [PubMed]
5. Sato, A.; Okubo, S.; Asai, K.; Ishii, S.; Mizutani, K.; Sugimoto, N. Stable dual-wavelength Q-switched Nd:YAG laser using a two-step energy extraction technique. *Appl. Opt.* **2015**, *54*, 3032–3042. [CrossRef]
6. Shang, L.H.; Wen, Y.; Li, T.Y.; Guo, Y.Y.; Wang, Y.H.; Wu, C.T.; Wang, C.; Jin, G.Y. Pulse peaks synchronize dual-wavelength laser based on Q-switch delay trigger. *Infrared Phys. Technol.* **2021**, *116*, 103751. [CrossRef]
7. Chang, W.K.; Chen, Y.H.; Chang, J.W. Pulsed orange generation optimized in a diode-pumped $Nd:YVO_4$ laser using monolithic dual PPLN electro-optic Q switches. *Opt. Lett.* **2010**, *35*, 2687–2689. [CrossRef]
8. Chen, Y.H.; Huang, Y.C. Actively Q-switched $Nd:YVO_4$ laser using an electro-optic periodically poled lithium niobate crystal as a laser Q-switch. *Opt. Lett.* **2003**, *28*, 1460–1462. [CrossRef]
9. Mo, J.; Chen, Y.; Li, R. Silver jewelry microanalysis with dual-pulse laser-induced breakdown spectroscopy: 266 + 1064nm wavelength combination. *Appl. Opt.* **2014**, *53*, 7516–7522. [CrossRef]
10. Coons, R.W.; Harilal, S.S.; Hassan, S.M.; Hassanein, A. The importance of longer wavelength reheating in dual-pulse laser-induced breakdown spectroscopy. *Appl. Phys. B* **2012**, *107*, 873–880. [CrossRef]
11. Diwakar, P.K.; Harilal, S.S.; Freeman, J.R. Role of laser pre-pulse wavelength and inter-pulse delay on signal enhancement in collinear double-pulse laser-induced breakdown spectroscopy. *Spectrochim. Acta Part B* **2013**, *87*, 65–73. [CrossRef]
12. Qiu, Y.; Wang, A.; Liu, Y.; Huang, D.; Wu, Q. The effect of inter-pulse delay on the spectral emission and expansion dynamics of plasma in dual-pulse fiber-optic laser-induced breakdown spectroscopy. *Phys. Plasmas* **2020**, *27*, 083516. [CrossRef]
13. Scaffidi, J.; Pender, J.; Pearman, W.; Goode, S.R.; Colston, J.; Bill, W.; Carter, J.C.; Angel, S.M. Dual-pulse laser-induced breakdown spectroscopy with combinations of femtosecond and nanosecond laser pulses. *Appl. Opt.* **2003**, *42*, 6099–6106. [CrossRef]
14. Zhang, M.; Wang, D.N.; Li, H.; Jin, W.; Demokan, M.S. Tunable dual-wavelength picosecond pulse generation by the use of two Fabry-Pe/spl acute/rot laser di-odes in an external injection seeding scheme. *IEEE Photonics Technol. Lett.* **2002**, *14*, 92–94. [CrossRef]
15. Lee, D.H.; Han, S.C.; Kim, T.H.; Yun, J.I. Highly sensitive analysis of boron and lithium in aqueous solution using dual-pulse laser-induced break-down spectroscopy. *Anal. Chem.* **2011**, *83*, 9456–9461. [CrossRef]
16. Zhou, Q.; Chen, Y.Q.; Peng, F.F.; Yang, X.J.; Li, R.H. Determination of ablation threshold of copper alloy with orthogonal dual-pulse laser-ablation la-ser-induced breakdown spectroscopy. *Appl. Opt.* **2013**, *52*, 5600–5605. [CrossRef]
17. Men, S.J.; Liu, Z.J.; Cong, Z.H.; Li, Y.F.; Zhang, X.Y. Electro-optically Q-switched dual-wavelength Nd:YLF laser emitting at 1047 nm and 1053 nm. *Opt. Laser Technol.* **2015**, *68*, 48–51. [CrossRef]
18. Wang, C.; Wen, Y.; Wang, Y.H.; Wu, C.T. 1064/1342 nm dual-wavelength double electro-optical Q-switched $Nd:YVO_4$ laser. *Opt. Commun.* **2021**, *479*, 126404. [CrossRef]
19. Degnan, J.J. Theory of the optimally coupled Q-switched laser. *IEEE J. Quantum Electron.* **1989**, *25*, 214–220. [CrossRef]
20. Sooy, W.R. The natural selection of modes in a passive Q-switched laser. *Appl. Phys. Lett.* **1965**, *7*, 36–37. [CrossRef]
21. Sato, A.; Okubo, S.; Asai, K.; Ishii, S.; Mizutani, K. Energy extraction in dual-wavelength Q-switched laser with a common upper laser level. *Appl. Phys. B* **2014**, *117*, 621–631. [CrossRef]

22. Oseledchik, Y.S.; Pisarevsky, A.I.; Prosvirnin, A.L.; Starshenko, V.V.; Svitanko, N.V. Nonlinear optical properties of the flux grown RbTiOPO$_4$ crystal. *Opt. Mater.* **1994**, *3*, 237–242. [CrossRef]

23. Koechner, W. *Solid State Laser Engineering*, 6th ed.; Springer: Berlin, Germany, 1976; pp. 499–514.

24. Yu, Y.J.; Chen, X.Y.; Wang, C.; Wu, C.T.; Yu, M.; Jin, G.Y. High repetition rate 880 nm diode-directly-pumped electro-optic Q-switched Nd:GdVO$_4$ laser with a double-crystal RTP electrooptic modulator. *Opt. Commun.* **2013**, *304*, 39–42. [CrossRef]

25. Yu, Y.J.; Chen, X.Y.; Wang, C.; Wu, C.T.; Liu, R.; Jin, G.Y. A 200 kHz Q-switched adhesive-free bond composite Nd:YVO$_4$ laser using a double-crystal RTP electro-optic modulato. *Chin. Phys. Lett.* **2012**, *29*, 207–210. [CrossRef]